Chemical Engineering Journal 161 (2010) 403–408

Contents lists available at ScienceDirect

Chemical Engineering Journal

journal homepage: www.elsevier.com/locate/cej

Mechanistic insights on the ethanol transformation into hydrocarbons over HZSM-5 zeolite

F. Ferreira Madeira[a,c], N.S. Gnep[a], P. Magnoux[a,*], H. Vezin[b], S. Maury[c], N. Cadran[c]

[a] LACCO, UMR6503, Université de Poitiers, 40, Avenue du Recteur Pineau, 86022 Poitiers Cedex, France
[b] LCOM, UMR8009, Université des Sciences et Technologies de Lille, bat C4 F, 59655 Villeneuve d'Asq, France
[c] Institut Français du Pétrole–Lyon, Rond-point de l'échangeur de Solaize, BP3, 69390 Vernaison, France

ARTICLE INFO

Article history:
Received 8 May 2009
Received in revised form
21 September 2009
Accepted 12 January 2010

Keywords:
Ethanol transformation
HZSM-5 zeolites
Radicals
EPR

ABSTRACT

HZSM-5 zeolite was found to be a very stable catalyst for the ethanol transformation into hydrocarbons at 350 °C and 30 bar total pressure. It was found to maintain high activity for C_{3+} hydrocarbons formation with time-on-stream in spite of a near total loss of Brønsted acidity, 92% loss of microporosity and high coke content deposited inside its micropore volume. The same solid, passivated with TEOS was tested in the same conditions and it was found that the treatment slightly improved the catalytic performance of the zeolite, even if similar losses of acidity and microporisty were determined after reaction. This shows that C_{3+} hydrocarbons' formation does not occur at the external surface. Alkyl aromatic hydrocarbons were found occluded in the zeolite structure after reaction, detected by IR spectroscopy analysis and by CH_2Cl_2 extraction after solubilization of the structure with HF solution. EPR-CW analysis of both coked samples proved existence of free radicals. This last technique could provide us further enlightening of the ethanol transformation mechanism.

1. Introduction

HMFI zeolite is a well-known catalyst for the transformation of methanol into olefins (MTO) [1] and gasoline (MTG) [2–4]. It is also one of the most studied and claimed as one of the best catalysts for ethanol transformation into ethylene (BTE) [5,6] and/or into higher hydrocarbons [7–9]. In methanol's case, the most appealing suggested mechanism nowadays is the hydrocarbon pool mechanism [10,11]. It has been shown that the adsorbate representing the hydrocarbon pool may have common characteristics with ordinary coke [11] and therefore a deeper study of the coke nature might help elucidating the C_{3+} hydrocarbons formation mechanism.

In our previous study [12], in comparison with HBEA and HFAU zeolites, having similar number of Brønsted acid sites, HMFI zeolite was also found to be the more stable and performing for ethanol transformation into C_{3+} hydrocarbons (particularly aliphatic and aromatic families). The best catalytic property of this zeolite is due to its capacity to maintain high activity in C_{3+} hydrocarbons with time-on-stream and this in spite of very low residual acidity and high coke content deposited inside its micropore volume.

In the present work, ethanol transformation into hydrocarbons was carried out on a HMFI zeolite having a large amount of Brønsted acid sites, its aim being to go thoroughly into the comprehension of the mechanism of these hydrocarbons' formation. In the 80s a free radical mechanism for the methanol transformation was suggested and supported by EPR evidence [13] but contested, for it remained unclear if they were essential to the reaction or not. It seems clear that a further study of the deactivation process and composition of the carbon deposit nature could be helpful to the enlightening of the ethanol transformation mechanism.

The subject of our work was approached by studying the nature of the products and of the carbonaceous species by using different spectroscopy techniques, such as IR and EPR analysis.

2. Experimental

HMFI (Si/Al ratio = 16) zeolite is a commercial material from Zeolyst International. The sample was compacted, crushed and sieved to achieve 0.2–0.4 mm homogeneous particles. Before catalytic testing, the solids were calcinated *in situ* under a nitrogen flow rate of 3.3 L h^{-1}, at 773 K and a total pressure of 30 bar.

Passivation of the external surface of the previously mentioned HZSM-5 zeolite was done using Tetra Ethyl Ortho Silicate (TEOS). The parent zeolite was previously calcinated at 823 K during 1 h under an air flow rate of 3 L h^{-1} per g of catalyst and then brought to ambient temperature. For the passivation procedure, the catalyst was heated at 423 K, under the same air flow rate as before. After 15 min at this temperature under nitrogen (flow rate 3 L h^{-1}

* Corresponding author. Tel.: +33 5 49 45 34 98; fax: +33 5 49 45 37 79.
E-mail address: patrick.magnoux@univ-poitiers.fr (P. Magnoux).

1385-8947/$ – see front matter © 2010 Elsevier B.V. All rights reserved.
doi:10.1016/j.cej.2010.01.026

per catalyst g), passivation started by bubbling the nitrogen into the TEOS solution (kept at 331 K) for 1 h. Then, pure nitrogen was passed for 15 min over the solid bed before heating up to 550 °C. The catalyst was then calcinated using the same conditions as before, for 4 h.

The ethanol used in the catalytic tests is a commercial product, from Carlos Erba (96%, V/V). It was used without any further purification.

Pore volumes of the fresh and coked catalysts were measured by nitrogen adsorption–desorption with a temperature program starting at 363 K (for 1 h) and rising up to 423 K (coked catalyst) or 623 K (fresh catalyst), under primary vacuum (2×10^{-3} torr) using an ASAP 2000 instrument (Micromeritics).

The acidity measurements were determined by pyridine adsorption followed by IR spectroscopy using a Nicolet Magna FTIR 550 spectrometer (resolution 2 cm^{-1}). In this case, the samples were first pressed into thin wafers (4–8 mg cm^{-2}) and activated *in situ* in the IR cell under secondary vacuum (10^{-6} mbar) at 623 K (fresh sample) and 423 K (coked samples). The estimation of acidity by pyridine adsorption was taken at 423 K using $\varepsilon_B = 1.13$ cm μmol^{-1} and $\varepsilon_L = 1.28$ cm μmol^{-1} as extinction coefficients for respectively Brønsted and Lewis acidities [14].

The CW X-band EPR spectra ($d\chi''/dB$) were recorded on a Bruker ELEXYS 580-FT spectrometer. Experimental technique was described elsewhere [15].

The carbon content of the coked catalysts was determined by complete combustion at 1293 K under helium and oxygen, using a Thermoquest NA2100.

2.1. Catalytic testing and products analysis

The catalytic tests were carried out in a continuous down-flow fixed bed reactor under a total nitrogen pressure of 30 bar. The reactor was made of stainless steel, 40 cm long with internal and external diameters of 1.3 and 1.7 cm, respectively. The catalyst (0.3 g) is placed in the middle of the reactor, between layers of glass balls of 1.19 mm diameter. Previous *in situ* activation was performed under nitrogen (30 bar, 3.3 L h^{-1}) for 16 h at 773 K. The gas flow was kept during reaction, while ethanol (96% V/V) was fed into the reactor at 2 ml/h, which corresponds to a N_2/ethanol molar ratio of 4 and a weight hourly space velocity (WHSV) of 15 h^{-1}. All tests were carried out at 623 K.

Reaction products were analyzed by on line gas-chromatography using a VARIAN 3800 gas chromatograph equipped with two detectors: a FID detector connected to a J&W PONA capillary column (100 m long, 0.25 mm of inner diameter and 0.5 μm of film thickness); and a TCD detector connected to a double column, composed of a 5A sieve (10 m long, 0.32 mm inner diameter and 10 μm of film thickness) plus a Porabond Q (50 m long, 0.53 mm inner diameter and 10 μm of film thickness). The reaction products' injection is made under pressure for the FID detector and at ambiance pressure to the TCD detector. The first one allows the detection of all hydrocarbons as well as the oxygenated compounds such as ethanol, diethyl ether or others. The other one allows the detection of hydrogen, nitrogen, carbon monoxide, carbon dioxide, oxygen and methane.

The oven programming starts at 20 °C (kept for 15 min) thanks to a cryogenic system and rises up to 250 °C, with different heating steps at 150 (kept for 10 min) and 220 °C (kept for 34 min), and with a heating rate of 8 °C/min.

In addition to the on-line analysis, the liquid and gas phases are also recovered and analyzed by GC-MS spectroscopy. Liquid phases (organic and aqueous) are also separated and weighted for mass balance purposes. Water content was determined by weighting the aqueous phase after phase's separation.

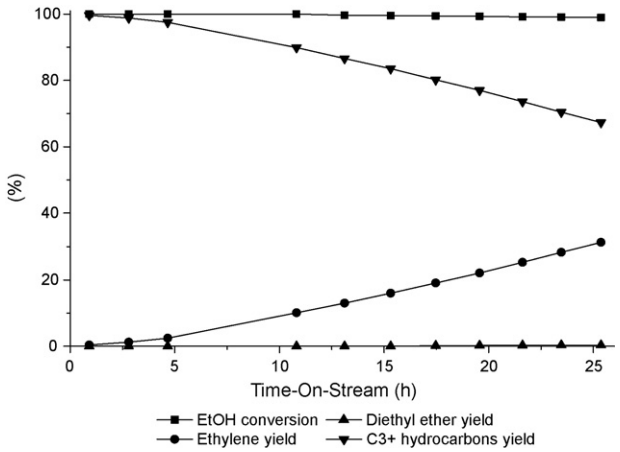

Fig. 1. Ethanol transformation on HZSM-5(16). Evolution of ethanol conversion and ethylene, diethyl ether and C_{3+} hydrocarbons yield with time-on-stream.

3. Results and discussion

Under our operating conditions ethanol was totally converted into ethylene, C_{3+} hydrocarbons, water (stoichiometric quantity from ethanol dehydration—about 39 wt%) and traces of diethyl ether (Fig. 1). Initially, ethanol is converted into ethylene and diethyl ether by dehydration reactions, followed by their transformation into higher hydrocarbons.

During all the run (25 h), no deactivation for ethanol conversion was observed. Ethylene began to be detected after 5 h of Time-On-Stream (TOS) and its quantity increased progressively with TOS, coinciding with the diminution of the C_{3+} hydrocarbons yield. Only trace amounts of diethyl ether were detected at the end of the run.

The results show that, even though there is no deactivation observed for the dehydration reaction, there is a deactivation towards the formation of higher hydrocarbons. It is widely accepted that deactivation on solid acid catalyst begins by eliminating the stronger Brønsted acid sites available [16]. If so, we can suppose that the formation of higher hydrocarbons requires stronger acid sites than ethanol dehydration.

For a better understanding of the reaction, we have decided to divide the C_{3+} hydrocarbons into three fractions according to the carbon number: C_3–C_4 (methane and ethane are produced in negligible amounts and ethylene was not taken into account being a primary product of ethanol dehydration and considered a reactant, as proposed in the literature [17]), C_5–C_{11}, C_{12+}; and also divided according to their chemical family: Paraffin, Olefin, Naphthene or Aromatic (PONA). Fig. 2 shows the evolution of the fractions' selectivity for three TOS of 0.9 (corresponding to the first analysis point), 13 and 25 h.

The C_5–C_{11} fraction was always largely superior, independent of time-on-stream. C_{12+} hydrocarbons were always detected in very small amounts and they are exclusively composed of aromatics. The amount of C_3–C_4 fraction was initially slightly lower than that of C_5–C_{11} (~1.2 times) and it continues to decrease with TOS (~2.4 times at TOS = 25 h) (Fig. 2). This could be due to high secondary cracking activity of the catalyst at the beginning of the reaction, due to the presence of stronger acid sites.

When studying the C_{3+} products selectivity by chemical family, we find a majority of paraffins and aromatics regardless of time-on-stream (Fig. 3). Nevertheless, at the end of the run, olefins gain in proportion. Initially, olefins and naphthenes are present in very small amounts, and the naphthenes quantity remains low during all the run. Olefin proportion increases with time, with the diminution of that of paraffins + aromatics. This means that at first, the catalyst is highly active for the hydrogen transfer reactions and its activity

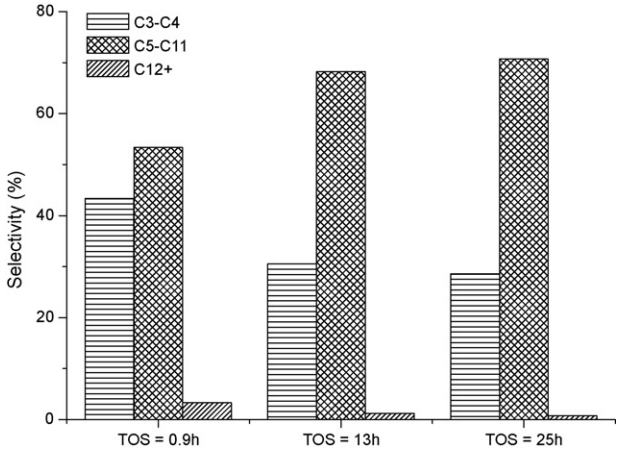

Fig. 2. Ethanol transformation on HZSM-5(16). Fractions selectivity, among C_{3+} hydrocarbons, for TOS = 0.9, 13 and 25 h.

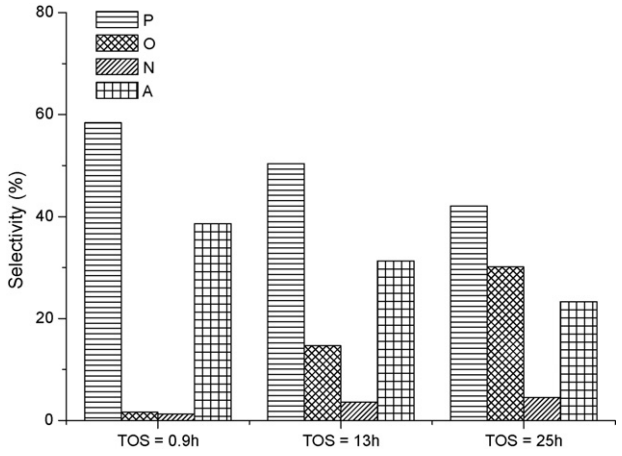

Fig. 3. Ethanol transformation on HZSM-5(16). Paraffins (P), olefins (O), naphtenes (N) and aromatics (A) selectivity, among C_{3+} hydrocarbons, for TOS = 0.9, 13 and 25 h.

decreases with its deactivation. Since the hydrogen transfer takes place between olefins to produce paraffins and aromatics, it is only natural that the selectivity in olefins increases with the diminution of hydrogen transfer reactions.

At the reaction beginning, propane, butanes and pentanes constitute the major products among paraffins. These compounds could result from the secondary cracking reactions (namely, the cracking of C_8 compounds), followed by hydrogen transfer reactions. Among olefins, butenes are the major products, representing 36 wt% of the olefins in the beginning and about 25 wt% at the end of the run. Among aromatics, C_8–C_{10} compounds represent 80–85% during all the run. Nearly all aromatics detected are highly alkylated benzenes. This is in agreement with the paraffin/aromatic molar ratio which is equal to three during all the run. In classic hydrogen transfer reactions, in order to form a single ring aromatic, three paraffins are formed (along with olefins consumption).

3.1. Characterization of the catalyst after reaction

Physical–chemical characterizations of the fresh HZSM-5(16) zeolite are summarized in Table 1. Its amount of Brønsted acid sites is twelve times greater than that of Lewis acid sites indicating that most of the aluminium atoms are in the structure. Its micropore volume represents about 70% of the total pore volume. As seen before (Fig. 1), there is a deactivation for the C_{3+} hydrocarbons formation over HZSM-5(16). This is probably due to coke deposit as can be seen from the high carbon content measured (∼9 wt%, Table 1). Coked HZSM-5(16) presents a near total loss of Brønsted and Lewis acidity. The coked sample was also nearly completely blocked, presenting a loss of 92% of its micropore volume.

The acidity measurements were first made using pyridine as a probe molecule, showing a 99.5% loss of Brønsted acidity. We have then used a smaller probe molecule, NH_3, to confirm these results and to have a probe molecule with a diameter closer to that of the ethanol molecule. The results reported in Table 1 show a 98% loss of total acidity, not far from the results obtained with pyridine. The IR spectra for the measurements using both probe molecules are shown in Fig. 4.

Coked HZSM-5(16) sample was first characterized by infrared spectroscopy (Fig. 5). Three main vibration bands regions of coke molecules were noted (Fig. 5a): 1620–1570 cm^{-1}, ∼1460 cm^{-1} and 1686–1370 cm^{-1}. According to the literature [18], bands in the first region were attributed to aromatic species; those in the second region to CH stretching $\delta_s(CH_2)$; and those in the third region to CH stretching $\delta_s(CH_3)$ and/or $\delta_s([CH_3]_2C<)$. This means that coke molecules occluded in the HZSM-5 zeolite structure are alkylaromatics. As can be expected, the presence of coke molecules neutralized OH– bridging acidic bands in the region around 3600 cm^{-1}, but also decreased the intensity of the silanol band (∼3740 cm^{-1}, Fig. 5b) which usually indicates the existence of external coke [19].

The carbon deposit was extracted using the method described by Guisnet in [20]. Not all of the occluded material could be retrieved. Coke molecules recovered by CH_2Cl_2 extraction were analyzed by GC-MS chromatography. The insoluble material was attributed to graphitic carbon. The chromatogram obtained for the soluble coke can be divided into two different regions. At the first part (Fig. 6a) mostly highly alkylated mono aromatics were found. These compounds were also detected on-line by GC analysis. At the second part (Fig. 6b), more condensed aromatics can be found, nevertheless they remain highly alkylated. These molecules are

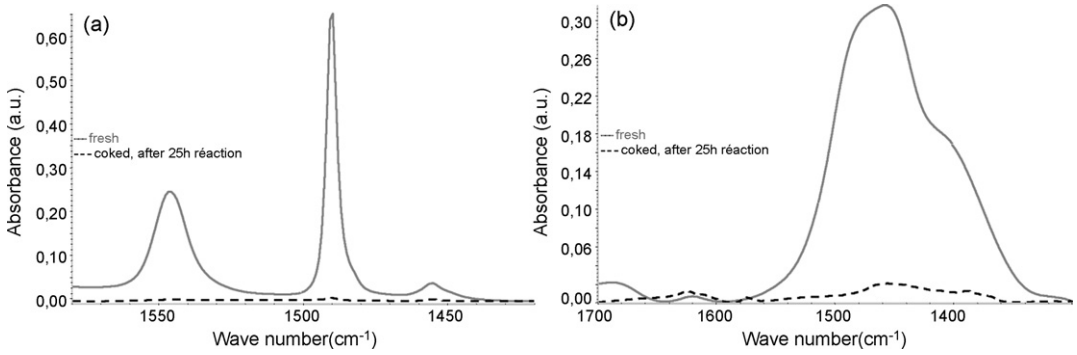

Fig. 4. IR spectroscopy analysis of fresh and coked HZSM-5(16), using pyridine (a) and NH_3 (b) as probe molecules.

Table 1
Physico-chemical characterization of fresh and coked HZSM-5(16) zeolite.

Catalyst sample	%C	Acidity[a] (probe: pyridine) (μmole/g)		Acidity[a] (probe: NH_3) (μmole/g)	Pore volume (cm^3/g)		
		Brønsted	Lewis	Total	Total	Micropore	Mesopore
HZSM-5 (16) fresh	–	608	50	645	0.267	0.184	0.083
HZSM-5 (16) after 25 h reaction	9.12	3	0	13	0.063	0.015	0.048

[a] Acidity measured at 150 °C; (xx) = Si/Al ratio.

probably responsible for the blockage of the zeolite micro porosity preventing the reactant access to the interior of the channel.

It must be kept in mind that at the end of the run, 100% of conversion of the ethanol is still reached and 67% of the products obtained are C_{3+} hydrocarbons, with a majority of paraffins and olefins belonging to the C_5–C_{11} fraction. Since there is practically no residual acidity, nor micro porosity left (Table 1), questions are raised to where and how the reactions occur. Furthermore, we have seen that among those C_{3+} hydrocarbons there are a majority of compounds belonging to the C_5–C_{11} fraction (Fig. 2), and a lot of aromatics (Fig. 3) still being formed. At this state of apparent deactivation (Table 1), it seems highly unlikely that the small remaining acidity measured can be responsible for the amount of hydrocarbons that are still being produced via, for instance, a carbocationic pathway, as proposed before by Palumbo et al. [21] when studying methanol conversion over HZSM-5, using spectroscopic techniques to characterize the carbon deposit. Also, micropore blockage is such that even if the acidity allowed bulky aromatics to be formed, it would be impossible for these compounds to come out. As a first guess we have assumed that, since there is no porosity left, the reactions could occur on the external surface and/or at pore mouth. To try to validate this hypothesis, we have submitted the catalyst to a passivation of the external surface by Tetra Ethyl Ortho Silicate (TEOS) in order to eliminate the acid sites available at surface. The catalyst was then submitted to the same characterizations as the parent zeolite, in terms of acidity and porosity. The catalytic testing was made in the exact same conditions as the previous one, and the results exploitation is similar.

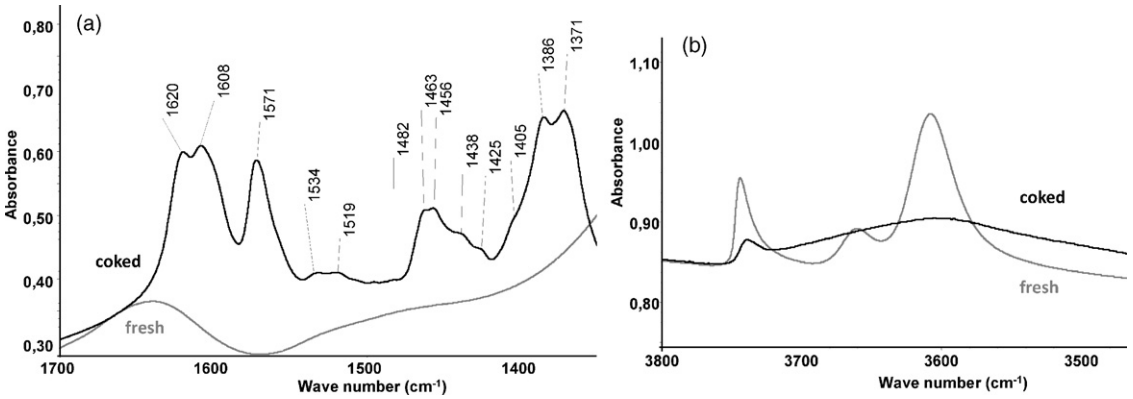

Fig. 5. IR spectroscopy analysis of coked HZSM-5(16). Vibration bands of coke molecules (a) and of silanol and OH bridging (b).

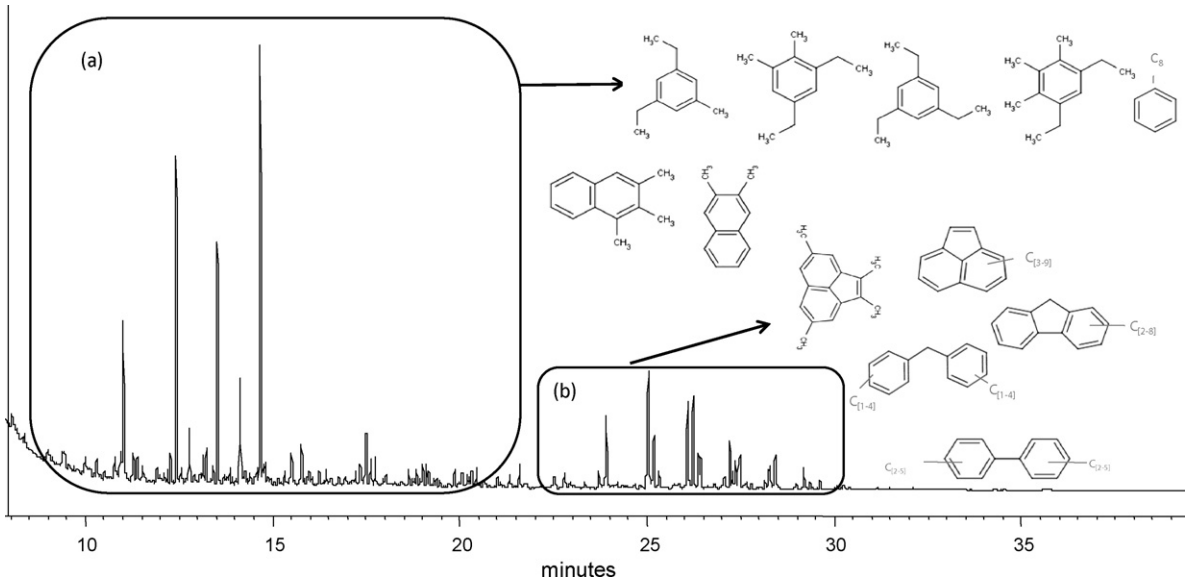

Fig. 6. GC-MS analysis of coke molecules extracted by CH_2Cl_2 after solubilization of coked HZSM-5(16) sample by HF solution.

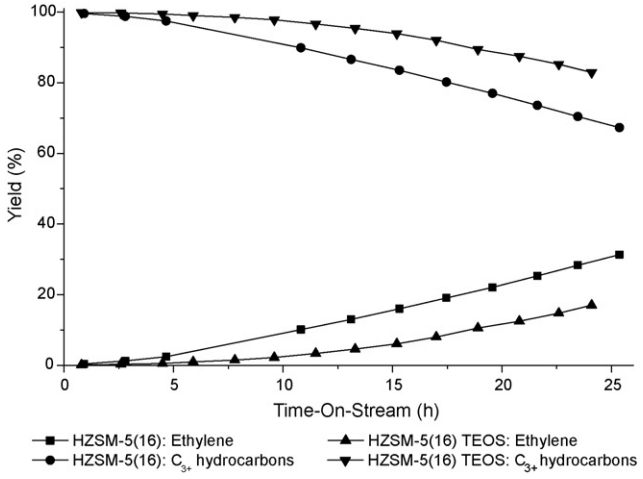

Fig. 7. Ethanol transformation on HZSM-5(16) and HZSM-5(16) passivated TEOS. Ethylene and C_{3+} hydrocarbons yield with time-on-stream.

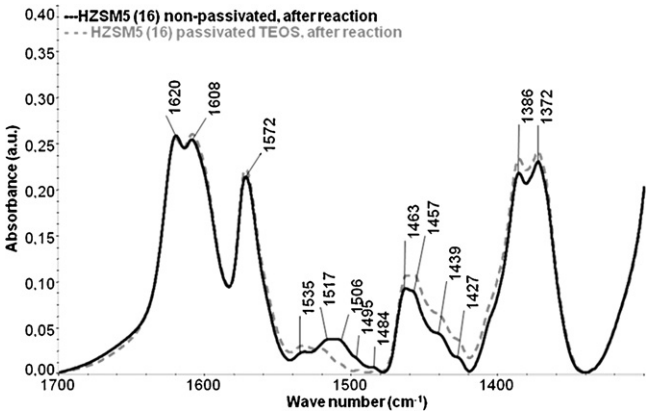

Fig. 9. IR spectroscopy analysis of coked HZSM-5(16) non-passivated and HZSM-5(16) passivated with TEOS, after 25 h reaction: vibration bands of the molecules composing the carbon deposit (coke).

3.2. Catalytic testing of a passivated HZSM-5 (Si/Al ratio = 16) zeolite

Once again, no deactivation was found for the ethanol transformation throughout all the run, nor was detected diethyl ether in amounts other than traces at the end. The results concerning the yield of ethylene and of C_{3+} hydrocarbons, for the parent catalyst and the passivated one are represented in Fig. 7 as a function of time-on-stream.

As we can see from Fig. 7, the passivated catalyst, for the same reaction time, presents a higher yield of C_{3+} hydrocarbons and a lower yield of ethylene than the ones found for the parent catalyst. After 25 h reaction the passivated sample presents a 23% higher yield of C_{3+} hydrocarbons.

Products selectivity for the different fractions (C_3–C_4; C_5–C_{11}; C_{12+}) and hydrocarbon families (PONA) are shown in Fig. 8. When comparing to the parent zeolite it can be seen that the passivation did not alter significantly the products' selectivity.

These results invalidate our previous hypothesis. The reaction clearly does not occur at the outer surface; nevertheless, and taking into account the microporosity loss, the reactions are almost certainly done at the pore entry of the channels of the catalyst, "pore mouth" catalysis.

In comparison with the parent zeolite, the passivated one presents a slightly lower Brønsted acidity and a slightly higher Lewis acidity (Table 2). There was practically no change in the pore volume of the HZSM-5 (16) after the passivation treatment (Table 2).

Coked HZSM-5(16) TEOS sample presented a loss of 98 and 73.5% of its initial Brønsted and Lewis acidity, respectively (Table 2). These results differ from the non-passivated coked sample ones (Table 1) where no residual Lewis acidity was measured. Once again, as remarked for the non-passivated coked HZSM-5(16) (Table 1), there was 89% loss of microporosity after 25 h on stream (Table 2). The IR spectra of the coke region for the non-passivated as well as the passivated HZSM-5 (16) coked samples, are shown in Fig. 9. We can see that we obtain exactly the same vibration bands with similar intensities for both samples. We therefore conclude that the

Table 2
Physico-chemical characterization of fresh and coked HZSM-5(16) passivated with TEOS zeolite.

Catalyst sample	%C	Acidity[a] (μmole/g)		Pore volume (cm^3/g)		
		Brønsted	Lewis	Total	Micropores	Mesopores
HZSM-5(16) TEOS fresh	–	560	83	0.262	0.176	0.086
HZSM-5(16) TEOS after 25 h reaction	9.24	11	22	0.071	0.020	0.051

[a] Acidity measured using pyridine as probe molecule, at 150 °C; (xx) = Si/Al ratio.

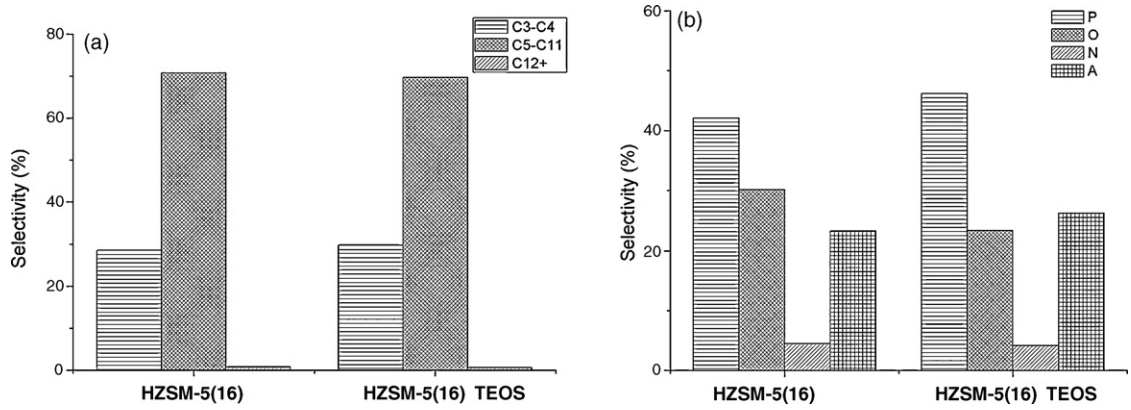

Fig. 8. Products selectivity among C_{3+} hydrocarbons for HZSM-5(16) and HZSM-5(16) TEOS zeolites, at TOS = 25 h. Distribution by fractions (a) and families (b).

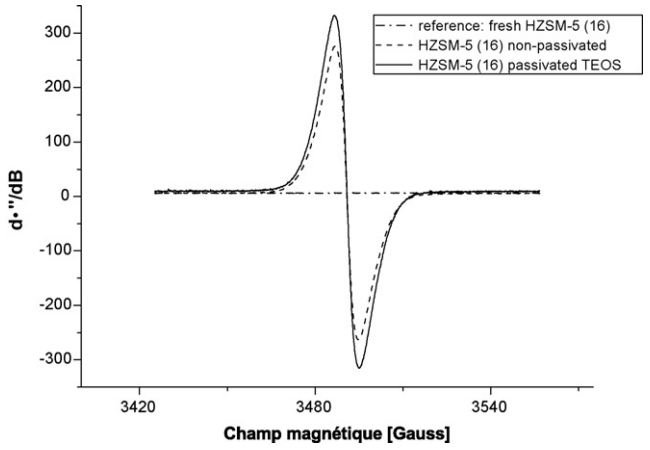

Fig. 10. EPR-CW analysis of HZSM-5(16) samples: fresh (-.-.-), after 25 h reaction non-passivated (- - -) and after 25 h reaction passivated TEOS (- - -).

occluded species composing the carbon deposit are the same for both samples.

From these results we are able to drawn the same conclusions as before (for the non-passivated sample), adding that the reactions do not seem to occur at the outer surface of the zeolites. In view of the catalytic activity presented by the catalyst when no residual acidity or micro porosity is measured, other questions concerning the nature and role of the species occluded in the structure (particularly at pore entry) are raised.

In order to deepen the mechanistic study of ethanol on HZSM-5 zeolites, EPR analysis of coked samples was undertaken. In the 80s, by using EPR analysis, it was reported that free radicals were detected on the reactions of dimethyl ether over HZSM-5 zeolite [13]. It was also shown that these free radicals and paramagnetic centres were present in the zeolite in tiny amounts as solid-state defects. They were proposed as a possible source of the activity in methanol/dimethyl ether transformation to hydrocarbons.

We have therefore decided to analyze the two coked HZSM-5(16) samples (the parent and the passivated zeolite) by EPR-CW technique.

The first results for the EPR-CW (Fig. 10) show the existence of an intense and well-defined paramagnetic signal and therefore, the existence of radicals in the two coked catalysts. The fresh sample serves as a reference and showed no signal. It can be seen that the passivated sample presents only a slightly higher intensity. The spin concentration of the samples is about 1.4×10^{18} spin/g of catalyst. Both signals present Lorentzien shapes with similar widths, which suggest a similar nature of the radical species.

These radicals could play an important role in the understanding of ethanol transformation into hydrocarbons. Nevertheless it remains to be established the activity or non-activity of these species to the hydrocarbons formation and if so, the importance of these reactions compared to the classical acid catalysis way. A radical mechanism could explain why solids which have lost almost all their acidity and porosity still catalyze the oligomerization of ethylene.

4. Conclusions

Ethanol transformation into hydrocarbons has been studied on HZSM-5 (16) zeolite passivated and non-passivated with TEOS. It was found that TEOS passivation slightly improves the catalytic properties of HZSM-5 (16) zeolite for C_{3+} hydrocarbon formation by limiting the deactivation of the catalyst. These zeolites presented high carbon content after 25 h reaction but they still keep high activity for C_{3+} hydrocarbon production, despite a near complete loss of Brønsted acidity and microporosity. Alkyl aromatic hydrocarbons were found occluded in the zeolite structure after reaction, detected by IR spectroscopy analysis and also by CH_2Cl_2 extraction after solubilization of the structure with HF solution. EPR-CW analysis of both coked samples found the existence of free radicals. This last technique could allow us in the future a deeper comprehension of the ethanol transformation mechanism.

References

[1] S.L. Meisel, Chemtech 18 (1988) 32–37.
[2] S.L. Meisel, J.P. McCullough, C.H. Lechthaler, P.B. Weisz, Chemische Technik 6 (1976) 86–89.
[3] C.D. Chang, A.J. Silvestri, J. Catal. 47 (1977) 249–259.
[4] C.D. Chang, Catal. Rev. 25 (1983) 1–118.
[5] W.R. Moser, R.W. Thompson, C.C. Chiang, H. Tong, J. Catal. 117 (1989) 19–32.
[6] R. Le Van Mao, T.M. Nguyen, G.P. McLaughlin, Appl. Catal. 48 (1989) 265–277.
[7] A.K. Talukdar, K.G. Bhattacharyya, S. Sivasanker, Appl. Catal. A 148 (1997) 357–371.
[8] A.G. Gayubo, A.M. Tarrio, A.T. Aguayo, M. Olazar, J. Bilbao, Ind. Eng. Chem. Res. 40 (2001) 3467–3474.
[9] N.R.C.F. Machado, V. Calsavara, N.G.C. Astrath, C.K. Matsuda, A. Paesano Junior, M.L. Baesso, Fuel 84 (2005) 2064–2070.
[10] I.M. Dahl, S. Kolboe, Catal. Lett. 20 (1993) 329–336.
[11] M. Stöcker, Micropor. Mesopor. Mater. 29 (1999) 3–48.
[12] F. Ferreira Madeira, N.S. Gnep, P. Magnoux, S. Maury, N. Cadran, Appl. Catal. A 367 (2009) 39–46.
[13] J.K.A. Clarke, R. Darcy, B.F. Hegarty, E. O'Donoghue, V. Amir-Ebrahimi, J.J. Rooney, J. Chem. Soc. Chem. Commun. (1986) 425–426.
[14] M. Guisnet, P. Ayrault, J. Datka, Polish J. Chem. 41 (1997) 1455–1461.
[15] M. Hureau, PhD thesis, Université des Sciences et Technologies de Lille, Lille, 2007.
[16] H.S. Cerqueira, P. Ayrault, J. Datka, P. Magnoux, M. Guisnet, J. Catal. 196 (2000) 149–157.
[17] V. Calsavara, M.L. Baesso, N.R.C. Fernandes-Machado, Fuel 87 (2008) 1628–1636.
[18] H.G. Karge, Coke formation on zeolites, in: H.G. Karge, E.M.F.H. van Bekkum, J.C. Jansen (Eds.), Introduction to zeolite science and practice, Elsevier, Amesterdam, 1991, pp. 531–570.
[19] P. Magnoux, P. Cartraud, S. Mignard, M. Guisnet, J. Catal. 106 (1987) 242–250.
[20] M. Guisnet, P. Magnoux, Appl. Catal. 54 (1989) 1–27.
[21] L. Palumbo, F. Bonino, P. Beato, M. Bjørgen, A. Zecchina, S. Bordiga, J. Phys. Chem. C 112 (2008) 9710–9716.